

Modelling and characterization of InP-based high-speed pin-photodiode

M. Nikoufard, X.J.M. Leijtens, Y.C. Zhu,
T.J.J. Kwaspen, E.A.J.M. Bente, F.H. Groen, M.K. Smit

COBRA, Eindhoven University of Technology
Den Dolech 2, P.O. Box 513, 5600 MB,
Eindhoven, The Netherlands
Tel. +31 40 2473649, Fax +31 40 2448375,
E-mail: M.Nikoufard@tue.nl

In this paper, the characteristics and a model of a side illuminated twin waveguide, pin-photodiode based on scattering parameters, is proposed. The equivalent small-signal model involves both the photodetector and the coplanar waveguide transmission line models. The measurement of the optoelectronic conversion parameter (S_{21}) of photodetector at $1.55 \mu\text{m}$ is done by an optical heterodyne technique which demonstrates 25 GHz bandwidths. The equivalent circuit model fits well with both the measured reflection (S_{22}) and the optoelectronic conversion parameter.

Introduction

For the design and development of high-speed optoelectronic systems and circuits, efficient and accurate models of optoelectronic devices such as laser diodes, light emitting diodes and photodiodes are required. Accurate characterization of the high-speed photodiode is essential to develop high-speed wideband optical devices [1–5]. At the same time, the accuracy of the models depends on the accuracy of the measurements. The modelling of the whole device allows us to investigate and understand the complex phenomena of optical and microwave interaction [4, 5, 7].

The first goal of this paper is to extract a model and the specifications of a side-illuminated twin waveguide pin-photodiode by output reflection-coefficient measurements. This can be achieved by performing measurements on wafer and fitting parameters of a suitable model to the measured data by software optimization [5]. The next goal is to characterize the photodetectors by an optical heterodyning technique and to compare the results with the extracted model [1–3]. The heterodyne measurement results are corrected for the effects of the relevant measurement systems. After these corrections we found good agreement between results obtained using two methods.

Pin-photodiode design, fabrication and modelling

Photodiodes with different lengths from $30 \mu\text{m}$ to $70 \mu\text{m}$ and width $8 \mu\text{m}$ were fabricated to analyse their RF behavior. A schematic view of the pin photodetector is depicted in figure 1. The structure of the pin-photodiode is based on a transverse twin-guide scheme. From the top down, the main parts of the pin-photodiode are a $400 \text{ nm } p^+ \text{-InP}$ contact layer, 100 nm InGaAs absorption layer, $100 \text{ nm non-intentionally doped}$ and $400 \text{ nm } n^+ \text{-InGaAsP(Q1.3)}$ layer, acting as the top waveguide layer and as n-contact layer. With this structure layer and $8 \times 60 \mu\text{m}^2$ area 0.25 pF can be achieved for a reverse bias voltage of 2 V and 0.12 pF for -5 V . The access waveguides consist of a 600 nm Q(1.3) layer with an InP cladding layer which is tapered from the normal width of $2 \mu\text{m}$ to $8 \mu\text{m}$ [6].

The devices were grown by low-pressure Metal Organic Vapor Phase Epitaxy (LP-MOPVE) at $625 \text{ }^\circ\text{C}$ on a semi-insulating InP substrate wafer to function at $1.55 \mu\text{m}$ wavelength. Ti/Au ($70 \text{ nm}/200 \text{ nm}$) are evaporated for the n- and p-contacts metallization. Next the mesa was defined by reactive ion etching (RIE) with $\text{CH}_4:\text{H}_2$ and subsequent $\text{HCL}:\text{H}_3\text{PO}_4$ solutions for InP and $\text{H}_2\text{SO}_4:\text{H}_2\text{O}_2:\text{H}_2\text{O}$ for InGaAs or InGaAsP, respectively. The isolation layer for the photodiodes is 100 nm SiN_x .

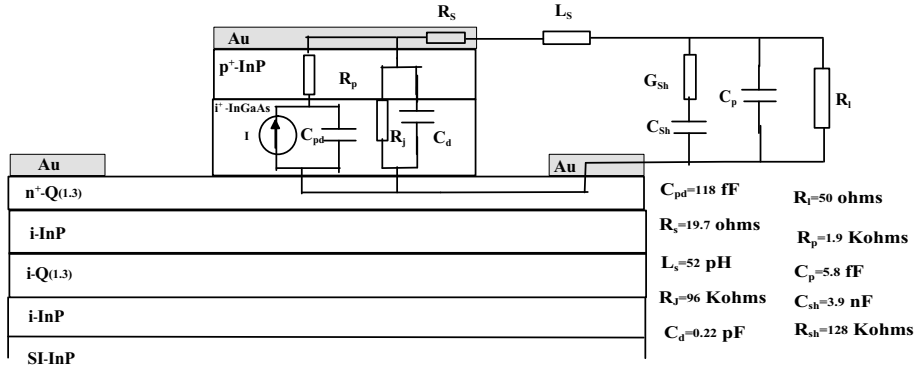


Figure 1: Cross section of a side-illuminated twin-waveguide pin-photodiode. The equivalent circuit elements represent physical parameters of the photodiode and parasitic elements.

Electrically, the output of the pin photodiode is fabricated as a coplanar waveguide transmission line in order to facilitate hybrid integration with the GaAs travelling-wave amplifier and also for on-wafer high-frequency measurements. Figure 1 indicates how the parasitic components are connected and how they are related to the physical parameters of the pin photodiodes. Here R_s is the p- and n-electrode contact resistance, R_j is the resistance representing the dark current leakage, R_p is the resistance of the bulk P^+ -InP layer; C_{pd} is the reverse-bias junction capacitance, C_d capacitance between p- and n-contact metallization which is significant at low frequencies, L_s is the inductance of the p/n-contacts to signal/ground electrodes, C_{sh} and G_{sh} are the shunt capacitance and conductance of coplanar waveguide which take into account the electric energy storage inside the transmission line and the losses caused by the transverse component, C_p is the open circuit at the end of the coplanar waveguide transmission line, and R_L is the load resistance.

Experimental results and discussion

To obtain the internal quantum efficiency and responsivity of photodiodes, light from a tunable laser source was coupled by a tapered lensed fiber into an optical waveguide at the AR-coated facet of the chip. The measured internal quantum efficiency for different pin-photodiodes are indicated in figure 2, which demonstrates that more than 90% of the optical power is absorbed by a diode of $60 \mu\text{m}$ length, coinciding with device simulations [6]. Using an exponential fitted function, photoabsorption of $\alpha=0.51 \text{ dB}/\mu\text{m}$ is found. A responsivity of approximately 0.70 A/W for $60 \mu\text{m}$ device length is calculated.

On-wafer network analyzer measurements are performed in the range of 50 MHz to 40 GHz without illumination to determine the parameters of a small signal equivalent circuit model from output reflection coefficient measurement. Figure 3 shows the measured and fitted S_{22} of a pin photodiode on a smith chart. The small signal equivalent circuit elements shown in figure 1 were extracted by the best fit of the measured S_{22} parameter across the measured frequency range for $60 \mu\text{m}$ length of the pin-photodiode. The R_s and C_{pd} for different lengths are shown in figure 4. The junction capacitance $C_{pd}=0.23\text{fF}/(\mu\text{m})^2$ was derived from photodiodes with different sizes. The average value of depletion thickness $d_{ave}=530 \text{ nm}$ is obtained from the junction capacitance ($d=\epsilon_0\epsilon_r A/C_{pd}$). In figure 5, the 3-bandwidth versus the device length is shown.

The frequency response of the fabricated pin-photodiodes is measured using an experimental setup for optical heterodyning with two tunable lasers [1, 2]. The beat frequency f_{RF} of the generated RF signal can be tuned by varying the wavelength of the one of tunable lasers ($\lambda_{tuned} = \lambda_0 \pm \Delta\lambda$

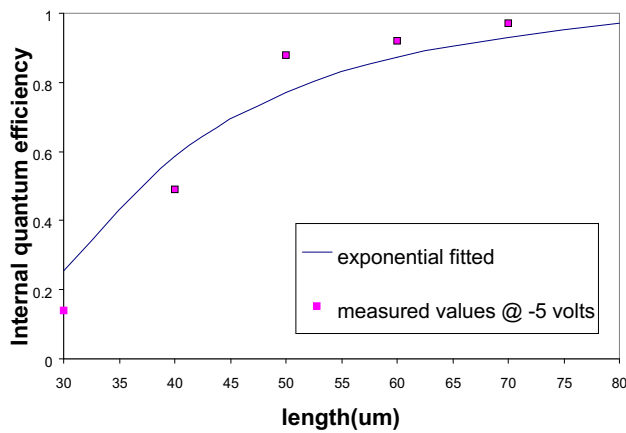


Figure 2: internal quantum efficiency for 8 μm wide waveguide photodiodes at 1550 nm.

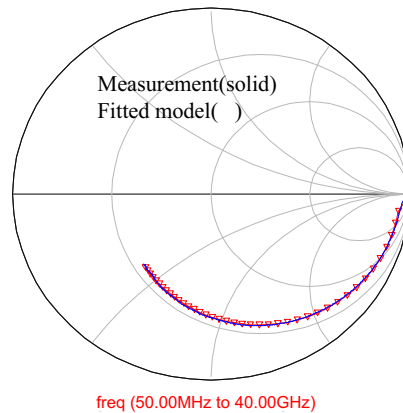


Figure 3: Measured and fitted S_{22} versus frequency of a pin-photodiode with 60 μm length on Smith Chart.

nm) while the wavelength λ_0 of the next tunable laser is fixed at 1550 nm.

$$f_{RF} = c \cdot \left(\frac{1}{\lambda_0} - \frac{1}{\lambda_{tuned}} \right)$$

where c is speed of light. Light from two tunable lasers is combined by a 3 dB optical coupler. The combined signals are amplified by a high power erbium doped (EDFA). In order to measure the total optical input power to the photodiode, the other output of the 3 dB coupler is connected to the power meter. A commercial coplanar probe with a bias-tee is connected to the electrode pads of photodiode. The photodiode is reversed biased using a DC power supply with photocurrent monitoring. The generated electrical signal is detected by a 40 GHz digital oscilloscope. The influence of the probe, RF connectors and cables, bias tee, and digital oscilloscope (50 Ω input resistance) obtained by a standard photodiode and used to calibrate the pin-photodiodes measured data. The loss due to electrical cables and probe is less than 1 dB at 40 GHz. The results of frequency response of the 60 μm device is presented in figure 6 which shows a 25 GHz bandwidth. The fluctuations in the frequency response is due to a mismatch between the probe and the bias tee. As shown in figure 6, by selecting the best values for the circuit elements shown in figure 1, the

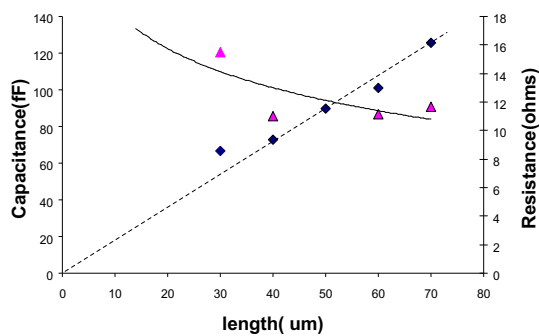


Figure 4: Capacitance (right) and resistance (left) calculated from S_{22} for different lengths.

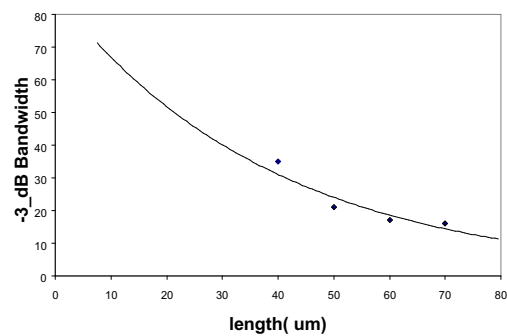


Figure 5: Measured bandwidth vs. length of pin-photodiodes.

calculated optical frequency responses (obtained from output reflection coefficient) can be fitted with the measured optical frequency response of the pin-photodiode at low-power-level small signal operation, where the photocurrent is below 1 mA.

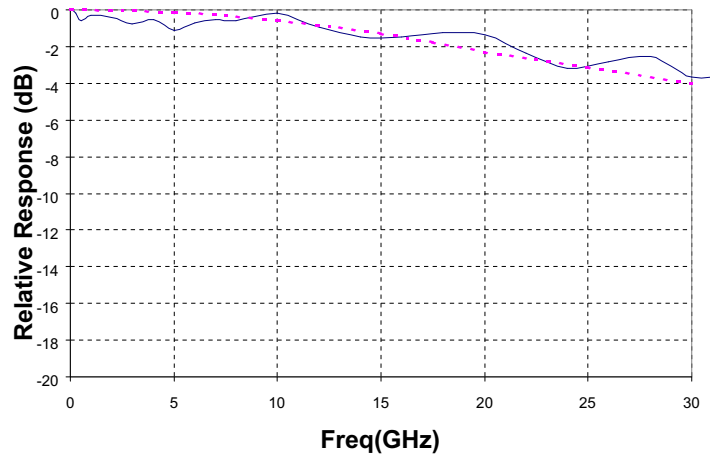


Figure 6: The measured relative frequency response of a 60 μm long pin-photodiode by a heterodyne technique (solid) and S_{21} obtained from fitted circuit (dot).

Conclusion

We have proposed a model for a twin-waveguide pin-photodiode with physical parameters. From the output reflection coefficient (S_{22}) of the pin-photodiode, the model parameters were extracted, which predict important device characteristics, such as the 3 dB and transit time bandwidths, the depletion region thickness, and the optical/electrical frequency response. The extracted characteristics have compared to experimental values obtained with heterodyning and other measurements techniques and were found to be in agreement. The fabricated pin-photodiodes have less than 5 nA dark current and more than 90% internal quantum efficiency and 25 GHz bandwidth for 60 μm length.

References

- [1] R.Thomas Hawkins II, M. D. Jones,S. H. Pepper, and J. H. Goll, "Comparison of fast photodetector response measurements by optical heterodyne and pulse response techniques," *J. Lightwave Technol.*, vol. 9, pp. 1289–1294, 1991.
- [2] S. Kawanashi, A. Takada, and M. Saruwatari," Wide-band frequency response measurement of optical receivers using optical heterodyne detection," *J. Lightwave Technol.* , vol. 7, No. 1,pp. 92–98, Jan. 1989.
- [3] P. Debie and L. Martens,"Correction technique for on-chip modulation response measurements of optoelectronic devices," *IEEE trans. on Microwave Theory Tech.*, vol. 43, no. 6, pp. 1264–1269, June 1995.
- [4] G. Unterborsch, A. Umbach, D. Trommer, G. G. Mekonnen,"70GHz long-wavelength photodetector," in *Proc. 28th Eur. Conf. on Opt. (ECOC '97)*, pp. 25-28, Sep. 22–25 1997.
- [5] G. Wang, T. Tokumitsu,I. Hanawa, Y. Yoneda, K. Sato, and M. Kobayashi," A time-delay equivalent-circuit model of ultrafast p-i-n photodiodes," *IEEE Trans. on Microwave Tech.*, vol. 51, No. 4, pp. 1227–1233, April 2003.
- [6] A. Siefke, M. Dahlstrom, U. Westergren, X. J. Leijtens, N. van Melick, and M. K. Smit,"Integration of an 8 \times 10 GHz polarization independent WDM receiver with HBT-preamplifiers," *proc. symp. IEEE/LEOS Benelux Chapter*, Gent, Belgium, pp. 25–28
- [7] A. Alping," Waveguide pin photodetectors: theoretical analysis and design criteria,"*IEE PROCEEDINGS*, vol. 136,Pt.J, No. 3, pp. 177–182, June 1989.